

Numerical simulation of the experiment of electrical explosion of aluminum foil

A V Shutov

Institute of Problems of Chemical Physics of the Russian Academy of Sciences, Academician Semenov Avenue 1, Chernogolovka, Moscow Region 142432, Russia

E-mail: shutov@icp.ac.ru

Abstract. Numerical simulation of the experiment of Korobenko *et al* (2007 *Phys. Rev. B* **75** 064208) in strongly coupled plasma of aluminum have been fulfilled. The results of numerical simulation and the experiment are compared. It is established that the hydrodynamic flows in the experiment can be assumed one-dimensional. The elastic-plastic effects in the dynamics of aluminum foil are also insignificant. The focus in the modeling is devoted to the study of the dynamics of the thermodynamic states of aluminum and their spatial homogeneity. It is emphasized the strong influence of the thermal conductivity for such experiments.

1. Introduction

By this numerical simulation, fields of pressure, density, temperature and velocity for one of experiments by Korobenko *et al* [1] were calculated. The experimental measurements have been performed on aluminum that expanded from the initial solid state by a factor of 6–9 under a supercritical pressure (> 10 kbar). Thin aluminum foil strip ($10 \mu\text{m}$) sandwiched between two ruby and two sapphire plates is heated by an electrical current pulse for less than $1 \mu\text{s}$, so that the Joule heat deposited into the sample achieves 4–6 the cohesion energy. One-dimensional (1D) numerical simulations of the similar experiments were presented in works [3, 4]. In the work [3], the thermal conductivity is absent in the model. In the work [4], there are thermal conductivity model, but the influence of thermal conductivity on the simulation results is not visible.

In the present work, the experimental and calculated pressure profiles give the same maximum pressure levels, and similar general view of the dependence of the pressure in time. It is shown that for this problem due to the small ($\sim 10 \mu\text{m}$) thickness of the foil and large ($\sim 1 \mu\text{s}$) time of measurement the thermal conductivity plays an important role. Due to the cooling of the aluminum foil surface, temperature and density distributions across the aluminum foil became not homogeneous. It is important to consider this fact for interpretation of experimental results.

2. Numerical modeling

The simulations fulfilled by two-dimensional (2D) hydrodynamic computer code BIG-2 [2]. This code is based on a Godunov type scheme that has a second order accuracy in space for solving the hydrodynamic equations. It uses a rectangular grid and includes heat conduction and uses equation-of-state for matter (EOS) data in tabular form of aluminum [5], SESAME model of sapphire [6, 7] and the same SESAME model of sapphire for ruby plates.



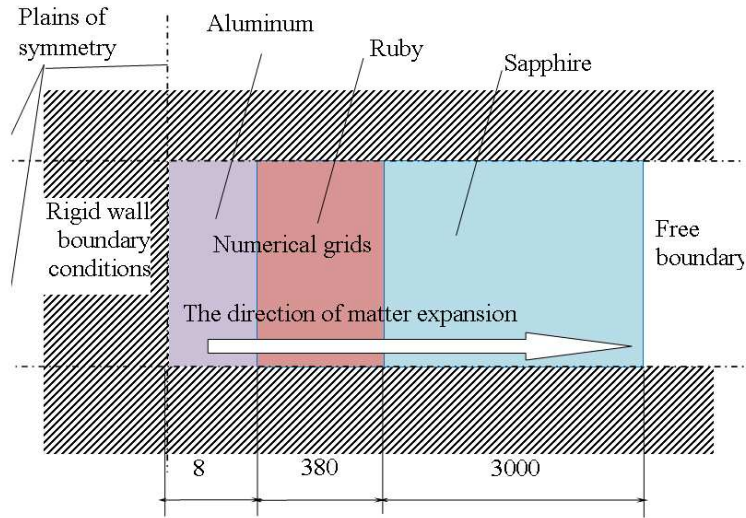


Figure 1. Scheme of the numerical grids location and the boundary conditions for 1D calculations by 2D code. The thicknesses of aluminum foil ruby and sapphire plates are shown by numbers in microns.

The complete system of equations describing unsteady elastic–ideal plastic behavior of a continuum written in the Cartesian coordinates for Euler variables has the form:

$$\rho_{,t} + (\rho u_i)_{,x_i} = 0, \quad (1)$$

$$(\rho u_i)_{,t} + (\rho u_i u_j - \sigma_{ij})_{,x_j} = 0, \quad (2)$$

$$e_{,t} + (e u_j - u_i \sigma_{ij})_{,x_j} - \lambda_T (T)_{,x_j, x_j} = \rho J_H, \quad (3)$$

$$D S_{ij} / Dt = 2\mu e_{ij}, \quad (4)$$

$$p = p(\varepsilon, \rho), \quad (5)$$

where a subscript “ $_{,y}$ ” denotes $\frac{\partial}{\partial y}$, t is time, $x_{i(i=1,2,3)}$ is space coordinates, u_i is velocity component for x_i coordinate, ρ is density, $e = \rho(\varepsilon + u_i u_i / 2)$ is energy per unit of volume, ε is specific energy per unit of mass, p is pressure, determined by equation of state (5), $\|\sigma_{ij}\|$ is stress tensor, which is divided into pressure and deviator stress parts: $s_{ij} = -p\delta_{ij} + S_{ij}$, $p = -\frac{1}{3}s_{ii}$, λ_T is thermal conductivity coefficient, J_H is Jule heat power (experimental data see fig.2), Sign D/Dt is used for the Jaumann derivative, which allows rotation of stress tensor in Euler variables, $D S_{ij} / Dt = S_{ij,t} + u_k S_{ij,x_k} - S_{ik} \omega_{jk} - S_{jk} \omega_{ik}$, where $\omega_{ij} = 1/2(u_{i,x_j} + u_{j,x_i})$, $\|e_{ij}\|$ is deviator of the tensor of the velocity of deformation tensor, $e_{ij} = \omega_{ij} - 1/3\omega_{kk}\delta_{ij}$, μ is the shear module.

The von Mises criterion for transition from elastic to plastic state is used: if $S_{ij} S_{ij} \geq \frac{2}{3}\sigma_S^2$, where σ_S is the yield strength of a material, then the components of the deviator stress are corrected by projecting them onto the yield surface, by multiplying them by $1/\sqrt{\lambda_t}$, where $\lambda_t = \frac{3}{2} \frac{S_{ij} S_{ij}}{\sigma_S^2}$. The yield strength is constant and taken as for solid under normal conditions while temperature less then melting point. For temperature higher then melting point, the yield strength drops to zero. For pure hydrodynamic case, the deviator parts of the stress tensor are equal to zero and equation (4) is excluded.

The initial data for 2D and 1D simulation correspond to the experiment. The 2D code is used also for 1D simulation. The experiment was carried out with aluminum foil with a thickness of $16\ \mu\text{m}$, a width of 6 mm, and a length of about 10 mm). The ruby plates (having a thickness of $380\ \mu\text{m}$, a width of 10 mm, and a length of 10 mm) together with the foil sample were sandwiched between two sapphire plates with a thickness of 3 mm. The symmetry of the experiment assembly is taken into account for the numerical simulation. In 1D case, the numerical region is limited by three straight lines with rigid wall boundary conditions. Two parallel straight lines are in horizontal direction and one vertical line drawn through the middle of the aluminum foil as shown on scheme figure 1. The numerical grid in this case is a linear sequence of rectangular cells. Every physical region with one material is covered by one numerical grid with Lagrange boundary conditions. The cell size in the horizontal direction is maintained at level $0.1\text{--}0.2\ \mu\text{m}$.

3. Numerical modeling results

Experimental dependence of deposited energy per gram of aluminum foil from time is taken as initial data for the numerical simulation. This energy deposition and calculated full energy of sample practically coincide. These are shown in figure 2. This coincidence demonstrates the conservatism of the calculation and the correctness of the numerical implementation of the energy input.

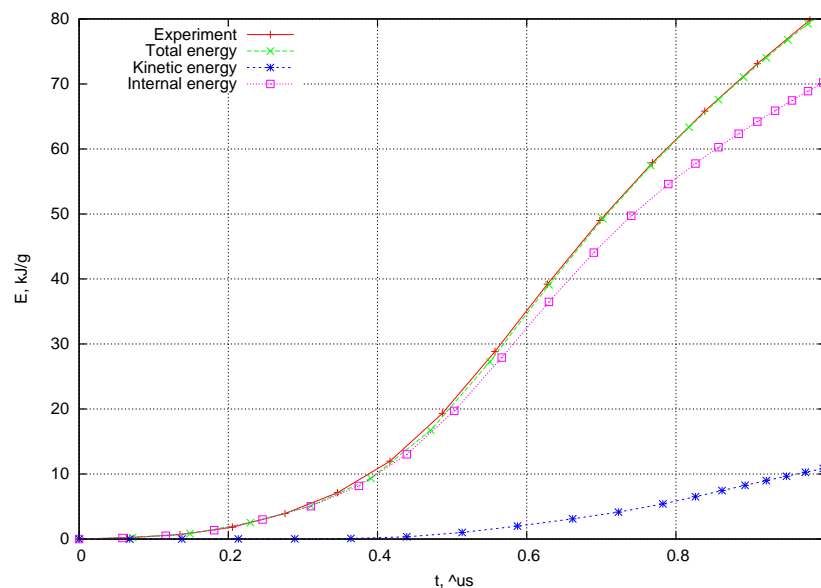


Figure 2. The energy in relation to 1 g of aluminum foil. Two upper lines are energy input by electrical current measured in the experiment and total energy of the sample in calculations. They almost coincide. The lowest line is kinetic energy of the sample by calculation. The middle one is internal energy of the sample.

2D calculations showed that the flow in the region of interest could indeed be regarded as 1D. Therefore, further calculations were performed in 1D case. The main experimental result is the dependence in time of pressure on aluminum surface. The experimental curve and the calculated one are similar and are shown on figure 3a for calculation with elastic-plastic and thermal conductivity and on figure 3b for pure hydrodynamics and without thermal conductivity.

It is seen in figure 3 that the calculated pressure profiles have similar time dependence as in the experiment and in both cases the calculations. Thermal conductivity does not affect on pressure on aluminum surface. Due to the small transverse size of the aluminum foil, which

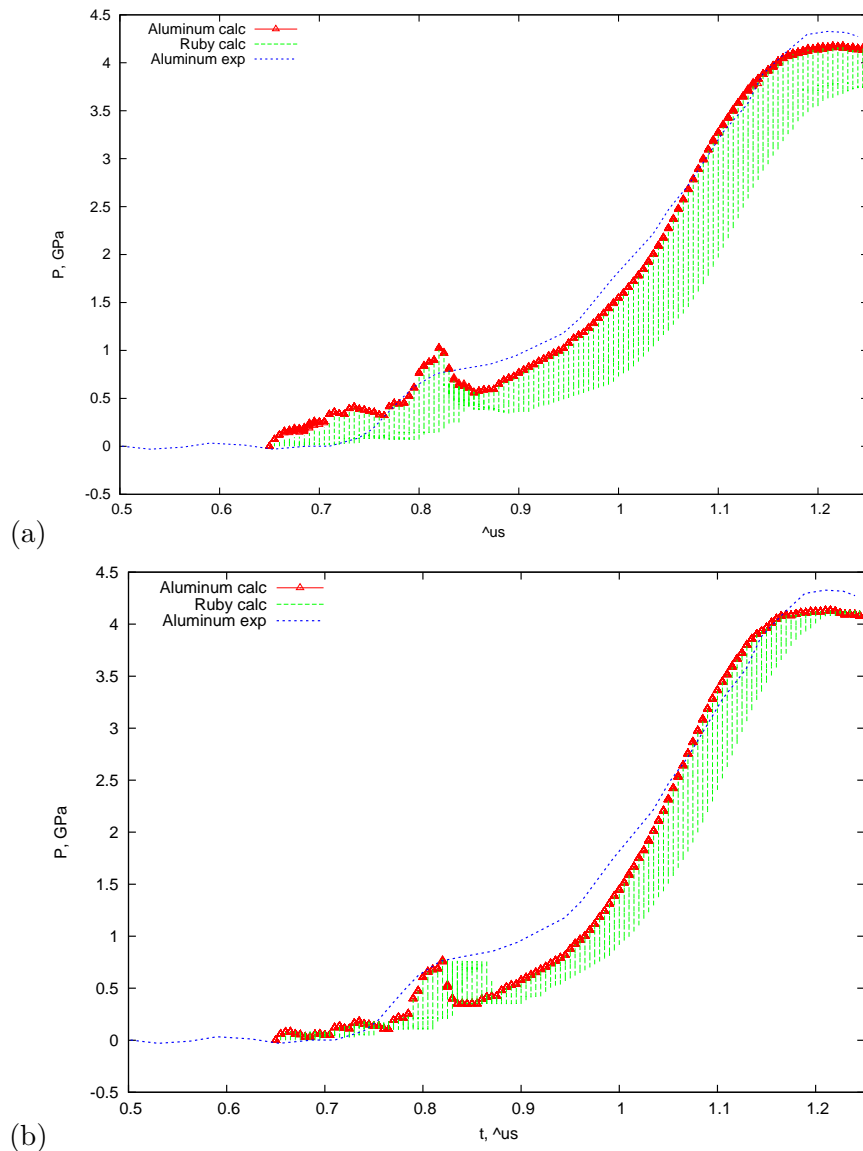


Figure 3. Calculated and measured pressure plots in time. Triangles are calculated pressure in aluminum foil. Vertical line segments are pressure distributed in ruby plate. Dashed line is experimental curve. (a) is variant of calculation with elastic-plastics and thermal conductivity. (b) is variant of calculation with pure hydrodynamics and without thermal conductivity.

is located between ruby plates and high sound speed the pressure in aluminum, is the same across the foil. However, pressure in ruby plates is distributed in space, and in the graphs it is represented by vertical segments of a straight line. The experimental pressure measurements are based on light wavelength shift in ruby and so these vertical segments represents uncertainty of the experimental pressure measurements.

The thermal conductivity does not affect on pressure distribution in aluminum foil but it is not so concerning density and temperature. Due to thermal conductivity, there are the temperature decrease and the density increase from the center to boundary of aluminum foil. Three-dimensional picture figure 4 shows the internal energy EOS surface together with calculated states for the aluminum foil.

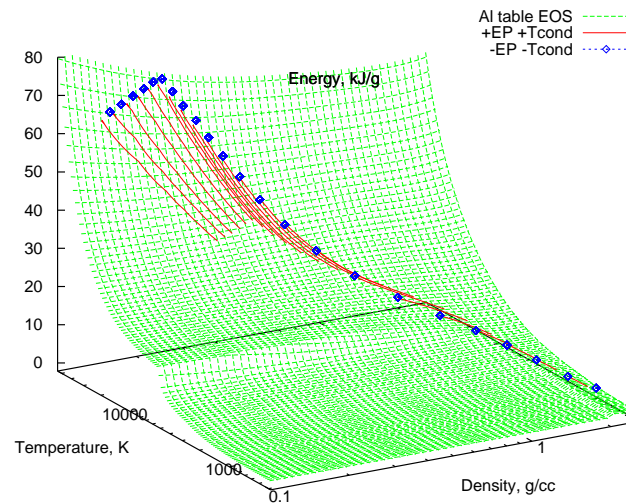


Figure 4. EOS of aluminum. Internal energy surface as function from density and temperature $\epsilon(\rho, T)$ together with states realized in calculations. Diamonds are states calculated without thermal conductivity with time steps 50 ns. Line segments are states calculated with thermal conductivity for the same time steps.

The data for every 50 ns time step plotted on the surface as open diamonds for case of calculation without thermal conductivity. In case of calculation with thermal conductivity, the plotted data are shown as line segments because the states are distributed across the depth of the aluminum foil. One can see that at the end of the electric energy release when the states in aluminum foil achieve high internal energy there are spread area of realized states presented by long line segments on the figure 4.

Another interesting feature that can be observed in the figure 4 is that, until the maximum internal energy, all thermodynamic states are almost on the one line. This means that at different times and in different parts of the foil are implemented the same thermodynamic states. Therefore, the coincidence of graphs in the thermodynamic coordinates for the different sections of the foil as in [3] does not prove the spatial homogeneity of the flow.

At the end, we present simple estimations of the thickness of the heat-conducting layer and the temperature on contact surface between foil and ruby plate for initially stepwise temperature distribution,

$$\delta_1 \simeq \sqrt{\frac{\lambda_1 \tau}{c_1 \rho_1}}, \quad (6)$$

$$T_b \simeq \frac{T_1 \sqrt{\lambda_1 c_1 \rho_1} + T_2 \sqrt{\lambda_2 c_2 \rho_2}}{\sqrt{\lambda_1 c_1 \rho_1} + \sqrt{\lambda_2 c_2 \rho_2}}, \quad (7)$$

where parameters of foil are marked by index 1 and parameters of contact plate are marked by index 2, for temperature the indexes mark values of the correspondent temperature steps. δ is a characteristic thickness of the heat-conducting layer, T_b is temperature of contact surface, τ is a characteristic time of the thermal conductivity process, λ is thermal conductivity coefficient, c is specific heat capacity, ρ is density.

Formula (7) shows that in the layer of δ_1 there is a continuous set of thermodynamic states in interval from T_b to T_1 , depending only on the degree of heating of the foil and the ratio of

Table 1. Material data and estimations.

Material	c , J/kg/K	ρ , kg/m ³	R , $\mu\Omega\text{m}$	λ , W/m/K	$K_{\lambda c\rho}$	δ , μm
Sapphire	761	3980	—	25	—	—
Aluminum	930	2700	15	81.3	0.62	2.5
Tungsten	134	19300	20	61	0.59	2.2

material constants on both sides of the contact. Time affects only the thickness of this layer. If T_1 much higher T_2 instead of (7), one may use:

$$T_b \simeq K_{\lambda c\rho} T_1, \quad (8)$$

$$K_{\lambda c\rho} = \frac{\sqrt{\lambda_1 c_1 \rho_1}}{\sqrt{\lambda_1 c_1 \rho_1} + \sqrt{\lambda_2 c_2 \rho_2}}. \quad (9)$$

The thermal conductivity coefficient is determined by Wiedamnn–Franz law:

$$\lambda = \frac{LT}{R}, \quad (10)$$

where L is Lorentz factor taken as $2.44 \times 10^{-8} \text{ W}\Omega\text{K}^{-2}$, R is resistivity.

Table 1 shows the data corresponding to the conditions of experiments, data on the electrical conductivity taken from these experiments and the obtained estimates. Parameters are $T_1 = 50000 \text{ K}$, $T_2 = 1000 \text{ K}$, $\tau = 0.3 \mu\text{s}$. The estimations are in good agreement with results of numerical simulations. From estimations $K_{\lambda c\rho}$ one conclude that T_b is about 60% of T_1 . In the work [4], to explain the electrical breakdown, the authors were forced to assume the availability of a much greater electrical conductivity in the surface layer of tungsten foil with a thickness about $0.5 \mu\text{m}$. The formation of such a layer is quite explainable by phenomenon of heat conduction. One can see that estimation of a characteristic thickness of the heat-conducting layer for tungsten is $2.2 \mu\text{m}$ and drop of temperature on 40%.

4. Conclusions

Good correspondence between experimental and numerical results shows that evaluable EOS and numerical simulation models give adequate description of the matter behavior for the experiments under consideration.

For the considered experiments, one should take into account the distribution of temperature and density caused by the phenomenon of thermal conductivity.

References

- [1] Korobenko V N and Rakhel A D 2007 *Phys. Rev. B* **75** 064208
- [2] Fortov V E, Goel B, Munz C-D, Ni A L, Shutov A and Vorobiev O Yu 1996 *Nucl. Sci. Eng.* **123** 169–89
- [3] Tkachenko S I, Levashov P R and Khishchenko K V 2006 *Czech. J. Phys.* **56** B419–24
- [4] Tkachenko S I, Levashov P R and Khishchenko K V 2006 *J. Phys. A: Math. Gen.* **39** 7597–7603
- [5] Fortov V E, Khishchenko K V, Levashov P R and Lomonosov I V 1998 *Nucl. Instrum. Meth. Phys. Res. A* **415(3)** 604–8
- [6] SESAME 1992 *LANL report LA-UR-92-3407*
- [7] Barnes J F and Lyon S P 1987 *LANL report LA-11058-MS*